The Interleukin-11 Receptor α as a Candidate Ligand-Directed Target in Osteosarcoma: Consistent Data from Cell Lines, Orthotopic Models, and Human Tumor Samples

Valerae O. Lewis,[1] Michael G. Ozawa,[2] Michael T. Deavers,[3] Guiying Wang,[1] Tomo Shintani,[4] Wadih Arap,[2] and Renata Pasqualini[2]

[1]Section of Orthopedic Oncology, Department of Surgical Oncology, [2]David H. Koch Center, and Departments of [3]Pathology and [4]Radiation Oncology, The University of Texas M. D. Anderson Cancer Center, Houston, Texas

Abstract

The interleukin-11 receptor α (IL-11Rα) is a functional target in bone metastasis. However, its role in primary bone tumors has not been established. As such, here, we evaluated IL-11Rα as a candidate target in primary and metastatic human osteosarcoma. First, in an orthotopic mouse model, we showed that IL-11Rα protein is markedly expressed in primary osseus and pulmonary metastatic osteosarcoma but absent from control normal tibia and lung. Moreover, systemic administration of an IL-11Rα–targeting phage displaying the cyclic nonapeptide CGRRAGGSC resulted in strong and selective accumulation of IL-11Rα–homing phage particles in the osteosarcoma but not in several control organs. Finally, IL-11Rα expression in a large panel of human primary and metastatic osteosarcoma samples was remarkably consistent with the observations in the orthotopic mouse model. These data establish IL-11Rα as a candidate target in human osteosarcoma and provide leads for the development of novel imaging and therapeutic agents for the management of this malignant tumor. [Cancer Res 2009;69(5):1995–9]

Introduction

Human osteosarcoma is the most common primary malignant tumor of bone (1). Although the introduction of modern chemotherapy has improved the 5-year survival to nearly 70%, hearing loss, cardiomyopathy, neuropathy, and renal failure are seriously debilitating and even fatal side effects of the systemic combination cytotoxic chemotherapy currently used (2, 3). Furthermore, tumors often respond to chemotherapy, but ultimately, many patients succumb to respiratory failure secondary to progression of pulmonary metastases. Investigators have evaluated many alternatives for selective therapy, including tyrosine kinase inhibitors, insulin-like growth factor-I inhibitors, radionucleotides, gene therapy, and monoclonal antibodies such as disialoganglioside GD2 and gp58 (refs. 4–9). However, these newer noncytotoxic treatments either lack systemic specificity or have limited efficacy against human sarcomas; thus, additional treatment options for this tumor is clearly an unmet need.

Molecular heterogeneity of the vascular endothelium enables selective targeting of agents to normal or diseased tissues (10, 11). Combinatorial approaches, such as *in vivo* phage display library selection, allow for interrogation of the endothelial cell surface in their native microenvironment and identification of targeting peptide motifs suitable for ligand-directed delivery (12). In previous work, we screened a phage display library in a human subject and reported a nonrandom peptide distribution (13–15). One of the selected ligand peptides contained the targeting motif Arg-Arg-Ala-Gly-Gly-Ser (RRAGGS, single-letter code) and exhibited similarity to human interleukin-11 (IL-11). This IL-11 mimic peptide bound the IL-11 receptor α (IL-11Rα), through a previously unrecognized binding site (16), and localized to the vasculature of human prostate cancer (13). Moreover, evaluation of IL-11Rα expression in an expanded set of clinically annotated prostate cancer samples has also shown a strong increase and gradual epithelial expression of IL-11Rα with concomitant pathologic progression to bone metastases (17). On an unrelated line of evidence, IL-11/IL-11Rα binding and downstream signaling via signal transduction and activator of transcription 3 activation has been proposed as a leading molecular pathway in metastasis (18).

In the present study, given the high expression of IL-11Rα protein and the proposed role of IL-11/IL-11Rα signaling in bone metastasis, we hypothesized that IL-11Rα similarly serves as a candidate target for primary and metastatic osteosarcoma. Using morphologic and functional analyses, we first examined a panel of mouse and human osteosarcoma–derived cell lines to establish the presence of a functional IL-11Rα protein. In animal models of osteosarcoma, we then showed that IL-11Rα within the bone microenvironment is accessible to a circulating particle displaying a mimic of the native ligand, IL-11, and strongly accumulates within the tumor. Finally, we showed that human primary osteosarcoma and pulmonary metastases express IL-11Rα, both in tumor cells and activated tumor blood vessels, while sparing normal bone marrow and lung. Together, these data indicate for the first time that IL-11Rα is a candidate target in human osteosarcoma and may serve as a target for ligand-directed delivery of agents against this disease.

Materials and Methods

Cell culture. Osteosarcoma cell lines derived from human (KRIB and OS187) and mouse (Dunn-LM, K7M3) were grown in DMEM containing 10% FCS, sodium pyruvate, streptomycin, nonessential amino acids, and multivitamins (4, 19).

Flow cytometric analysis of IL-11Rα expression. Osteosarcoma cells were plated at 8×10^5 cells. After 24 h, cells were trypsinized, suspended in a fluorescence-activated cell sorting buffer consisting of PBS, 2% FCS, and 0.1% NaN_3, and incubated with either 1 mg/mL phycoerythrin

Note: Supplementary data for this article are available at Cancer Research Online (http://cancerres.aacrjournals.org/).

Requests for reprints: Valerae O. Lewis, Wadih Arap, or Renata Pasqualini, The University of Texas M. D. Anderson Cancer Center, 1515 Holcombe Boulevard, Houston, TX 77030. Phone: 713-792-3873; Fax: 713-745-2999; E-mail: volewis@mdanderson.org, warap@mdanderson.org, or rpasqualini@mdanderson.org.

doi:10.1158/0008-5472.CAN-08-4845

(PE)-conjugated hamster anti-mouse IL-11 monoclonal antibody or isotype-matched, PE-conjugated control hamster IgG antibody (Pharmingen) for 30 min at 4°C. Samples were washed and analyzed by flow cytometry (FACScan; Becton Dickinson).

Cell internalization assay. Internalization assays were performed as described (17). In brief, osteosarcoma cells were plated overnight on 6-well polystyrene plates to a concentration of 5×10^4 cells/2 mL medium. Cells were blocked with 500 μL of DMEM containing 30% FCS for 60 min at 37°C then incubated with 10^9 transducing units (TU) of phage in DMEM containing 2% FCS for 4 h at 37°C. Cells were sequentially washed with PBS containing 10% bovine serum albumin (BSA), glycine buffer, PBS, and then fixed with PBS containing 4% paraformaldehyde (PFA). Cells were permeabilized with PBS containing 0.2% Triton X-100 (5 min at room temperature; RT), extensively washed with PBS, and blocked with PBS containing 5% normal serum and 1% BSA for 2 h at RT. The cells were incubated with a rabbit antiphage antibody (Sigma; 1:500 dilution) in PBS containing 1% normal serum (2 h at RT) and washed with PBS. Primary antibodies were detected with a Cy3-conjugated anti-rabbit IgG (Jackson ImmunoResearch; 1:300 dilution) in PBS (1 h at RT), rinsed with PBS (1 min at RT), fixed with PFA (15 min at RT), and mounted with Vectashield (Vector Laboratories).

Intratibial implantation of osteosarcoma cells. Male athymic nu/nu (nude) mice were purchased from the animal production area of the National Cancer Institute-Frederick Cancer Research Facility and maintained in a pathogen-free barrier animal facility approved by the American Association for Accreditation of Laboratory Animal Care.

For intratibial administration, cultured osteosarcoma cells at 80% confluence were briefly washed with PBS and then detached with 0.25% trypsin and 0.02% EDTA. Cell detachment was stopped after 1 min with DMEM containing 10% FCS. Cells were washed once in serum-free medium and resuspended in Hank's buffered salt solution. Suspensions containing >90% viable (trypan blue–excluding) cells were used for administration. Cells were injected (5×10^4 cells per mouse) into the right tibia of 5-wk-old nude mice anesthetized with Nembutal (50 mg/kg i.p.). Tumor growth was monitored with a Faxitron MX-20 X-ray unit, and images were digitally captured. Mice were killed at 1, 3, 5, 7, and 8 wk postinjection. Tibias (experimental and contralateral) and visceral organs were collected and processed. Histopathology was used to evaluate the presence of tibial and/or pulmonary tumors.

Immunohistochemical analysis. Mouse osteosarcoma samples were stained within 2 wk of sectioning. Four-micrometer sections were subjected to antigen-retrieval by heat with EDTA (pH 8.0; Zymed) followed by biotin and protein blocking (DAKO). Cell expression of IL-11Rα protein was evaluated with a rabbit anti–IL-11Rα antibody (C20; Santa Cruz Biotechnology) that cross-reacts (human and mouse) with the receptor. Primary antibodies were diluted at 1:15 and incubated for 45 min followed by development with the LSAB+ kit (DAKO).

Dual staining for IL-11Rα and CD31. Tumor specimens were collected and analyzed for IL-11Rα and CD31 expression as described (20, 21). Briefly, frozen tissue cryostat sections were fixed in a 50:50 solution of alcohol and acetone for 15 min, then washed with PBS. Nonspecific proteins were blocked by incubation in 5% normal horse serum plus 1% normal goat serum in PBS for 20 min. Sections were incubated with an anti-CD31 primary antibody followed by a secondary antibody conjugated with Alexa 594 (Molecular Probes). Sections were blocked again with PBS containing 4% gelatin (Electron Microscopy Sciences) and washed with PBS. Protein expression of IL-11Rα was detected with an anti–IL-11Rα rabbit antibody (Santa Cruz), followed by a goat anti-rabbit antibody conjugated with Alexa 488 (Molecular Probes). Slides were counterstained with Hoechst 3222 and visualized under standard fluorescence microscopy.

Tumor targeting. Targeted phage experiments *in vivo* were performed as described (22–24). Briefly, male athymic nude mice bearing intratibial tumors were anesthetized and injected i.v. (tail vein) with 10^9 TU of CGRRAGGSC-displaying phage, RGD-4C phage (positive control), or an fd insertless phage (negative control). After 24 h, mice were systemically perfused through the heart with 20 mL of PFA. Tumor and control organs were removed and fixed in formalin. Tibial tumors underwent decalcification. Tissue samples were paraffin-embedded and sectioned into 4-μm specimens for staining (23).

IL-11Rα in human primary tumors and lung metastases. After Institutional Review Board approval, the osteosarcoma database and hospital tumor registry at the University of Texas M. D. Anderson Cancer

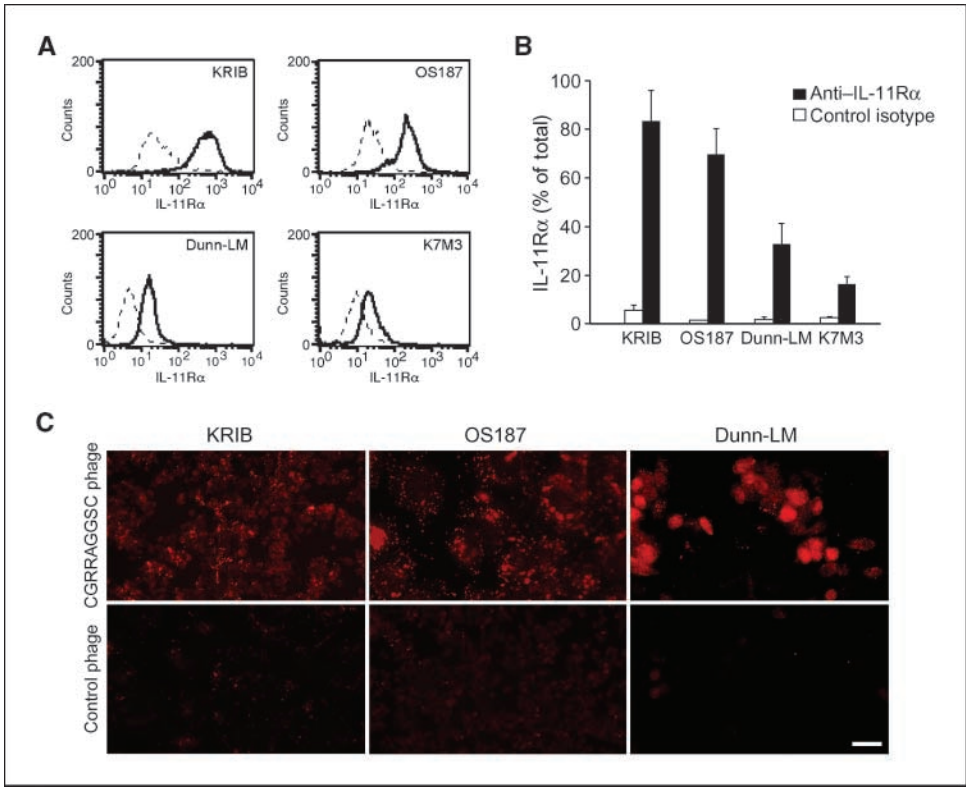

Figure 1. IL-11Rα protein expression in osteosarcoma cells. *A,* cells were labeled with either PE-conjugated polyclonal anti–IL-11Rα antibody (*solid bold line*) or PE-conjugated IgG isotype control (*dashed line*) and measured by flow cytometry. *B,* expression of IL-11Rα was statistically analyzed (*Sigma Plot*). The data represent mean values of three independent experiments (*t* test, $P < 0.05$). *C,* IL-11Rα–targeted peptides mediate receptor-ligand internalization. CGRRAGGSC-displaying phage or control insertless phage were incubated with osteosarcoma cell lines for 4 h at 37°C to allow targeted phage internalization. Internalized phage clones (*red dots*) were detected with an antiphage antibody after cell permeabilization. *Scale bar,* 30 μm.

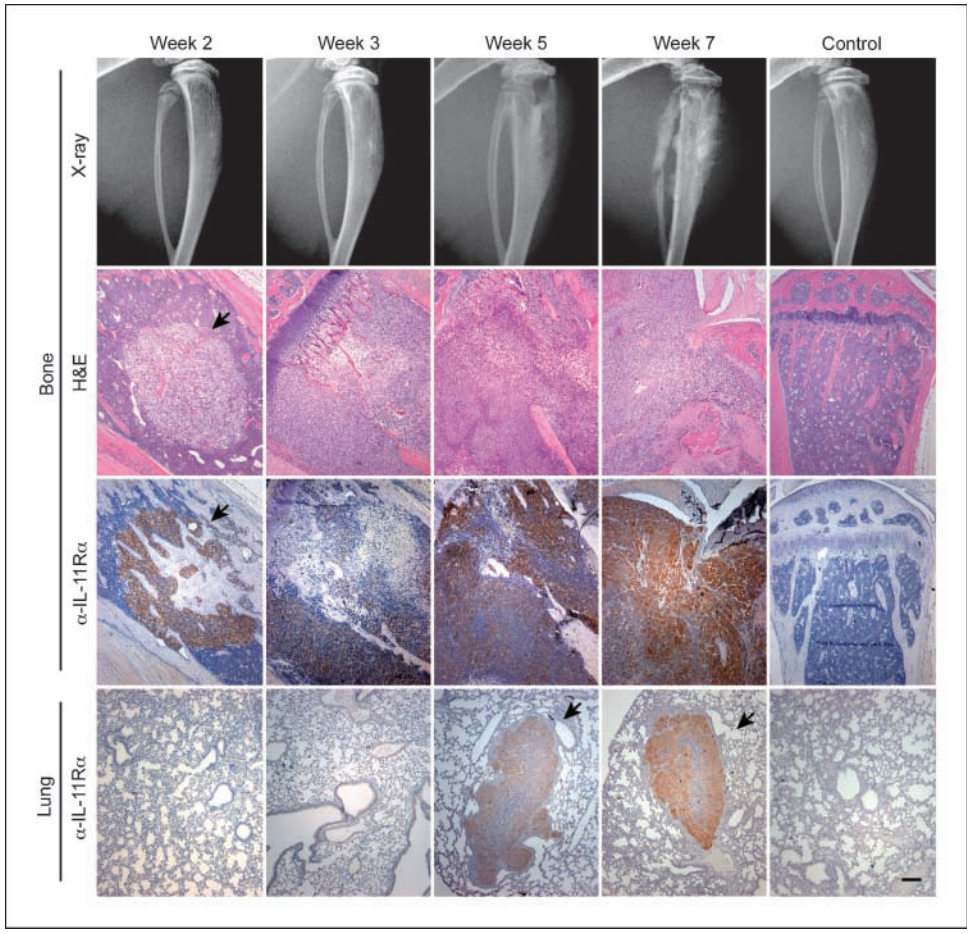

Figure 2. Serial radiographs and immunohistochemical analysis of IL-11Rα in tibial osteosarcoma and lung metastases. Radiograph of tibial osteosarcoma reproducibly shows progression of the lesion over time. A typical experiment is shown. At week 2, a cortically confined lesion is seen (*arrow*). At week 3, posterior breakthrough is noted. Week 5 shows longitudinal extension of the lesion with progressive bony destruction and posterior and anterior cortical breakthrough. Week 7 illustrates bony destruction and the classic sunburst pattern of periosteal reaction. In representative images of the tumors at 5 and 7 wk, the osteosarcoma have broken out anteriorly and posteriorly of the tibia. Control limbs show no visible lesion. Corresponding H&E staining and IL-11Rα expression of the tibial osteosarcoma lesions shows consistent expression of IL-11Rα with no expression in control normal bone (magnification, ×200). Lung sections stained for IL-11Rα expression show no expression in the control normal lung parenchyma but metastatic lesions express the receptor markedly. Pulmonary metastases were first detected at week 5 (*arrows*). *Scale bar,* 100 μm.

Center were queried from 2002 to 2007 for human osteosarcomas. Samples with <60% necrosis were then identified. From this specific query, primary bone samples (n = 30) and lung metastases (n = 19) were examined for the expression of the IL-11Rα. Slides with viable tumor were stained as detailed above. The specimens were graded for intensity of staining on a scale of 1 to 3 and for distribution on scale of 1 to 4 (Supplementary Fig. S1).

Results and Discussion

Osteosarcoma cells express IL-11Rα. To determine whether IL-11Rα would serve as a molecular target for osteosarcoma, we first evaluated the cell surface expression of IL-11Rα in several osteosarcoma cell lines. An anti–IL-11Rα antibody recognizing both human and mouse IL-11Rα showed positive reactivity of KRIB and OS187 (human) as well as Dunn-LM and K7M3 (mouse) cells (Fig. 1*A*). The data represent mean values of three independent experiments and are quantified (Fig. 1*B*). To further assess whether IL-11Rα is functionally active in osteosarcoma, we investigated the ability of KRIB, OS187, and Dunn-LM osteosarcoma cells to bind and internalize an IL-11 mimic peptide (17). Immunofluorescence analysis revealed that such CGRRAGGSC-displaying phage specifically bound and internalized into osteosarcoma cells, whereas an insertless negative control phage could not be detected under identical experimental conditions (Fig. 1*C*). These data support the expression of IL-11Rα on osteosarcoma cells and present a viable candidate target for ligand-directed delivery to tumor cells.

Systemic targeting of an orthotopic osteosarcoma model. *In vivo* models of osteosarcoma that spontaneously metastasize to the lung are robust and reproducible systems on which to not only study the mechanism of tumor growth and pulmonary metastases but also to assess the efficacy of potential antitumor and antimetastatic agents. There are several osteosarcoma cell lines that when injected orthotopically into the tibia develop evidence of clinical and radiographic osteosarcoma lesions (4, 19, 25). In addition, as in human osteosarcomas, these lesions can metastasize from the primary site into pulmonary metastases. The similarity of these rodent models to the natural history of osteosarcoma provide a valuable tool to rapidly translate newly identified molecular markers for clinical applications.

By using a representative panel of osteosarcoma cell lines (KRIB, OS187, Dunn-LM, and K7M3), we generated orthotopic, metastatic mouse models of osteosarcoma (4, 19). We established a time course of tumor development and monitored its burden by X-ray radiography. The histopathologic and experimental findings with each cell line were reproducibly similar. Therefore, we focused study on the KRIB cell–derived orthotopic model and studied the protein expression of IL-11Rα *in vivo* by immunohistochemistry in formalin-fixed, paraffin-embedded tissue samples at 2, 3, 5, and 7 weeks postinjection (Fig. 2). Beginning at an early time point (3 weeks), IL-11Rα staining was strongly localized to the intratibial lesion then limited to the periphery of the lesions observed at later time point s (6–8 weeks). This change in staining pattern suggested the IL-11Rα staining was most prominent in viable tumor areas, as the central areas of the tumors became necrotic. IL-11Rα expression in control normal bone (contralateral tibia) was barely

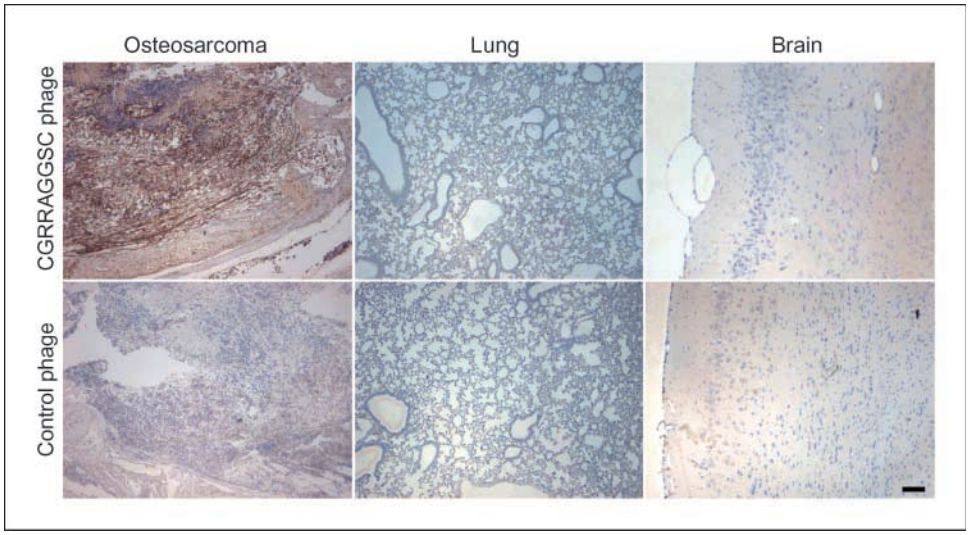

Figure 3. Systemic targeting of osteosarcoma by targeted phage. Immunohistochemical analysis of phage accumulation after i.v. administration of either CGRRAGGSC-displaying phage (*top row*) or insertless fd-tet negative control phage (*bottom row*) into mice bearing orthotopic osteosarcoma showed strong phage staining within the tumor, whereas the negative control was barely detectable above background. *Scale bar,* 100 μm.

detectable. Furthermore, at later time points, IL-11Rα was strongly expressed in pulmonary lesions with no expression detected in the control normal lung parenchyma (Fig. 2).

Having shown the presence of IL-11Rα in orthotopic models of osteosarcoma, we next sought to evaluate systemic targeting of IL-11 mimic–displaying phage particles to the osteosarcoma lesions. We i.v. administered either the CGRRAGGSC-displaying phage or the insertless negative control phage to mice bearing intratibial osteosarcomas. After 24 hours of circulation, the CGRRAGGSC-displaying phage showed strong staining within the tumors with little to no accumulation detected in several control organs by immunohistochemistry (Fig. 3, *top row*). In contrast, the insertless negative control phage were barely detectable in tumors (Fig. 3, *bottom row*). As previously well established (26, 27), phage were identified in the spleen and liver, which are part of the reticuloendothelial system that nonspecifically clear phage

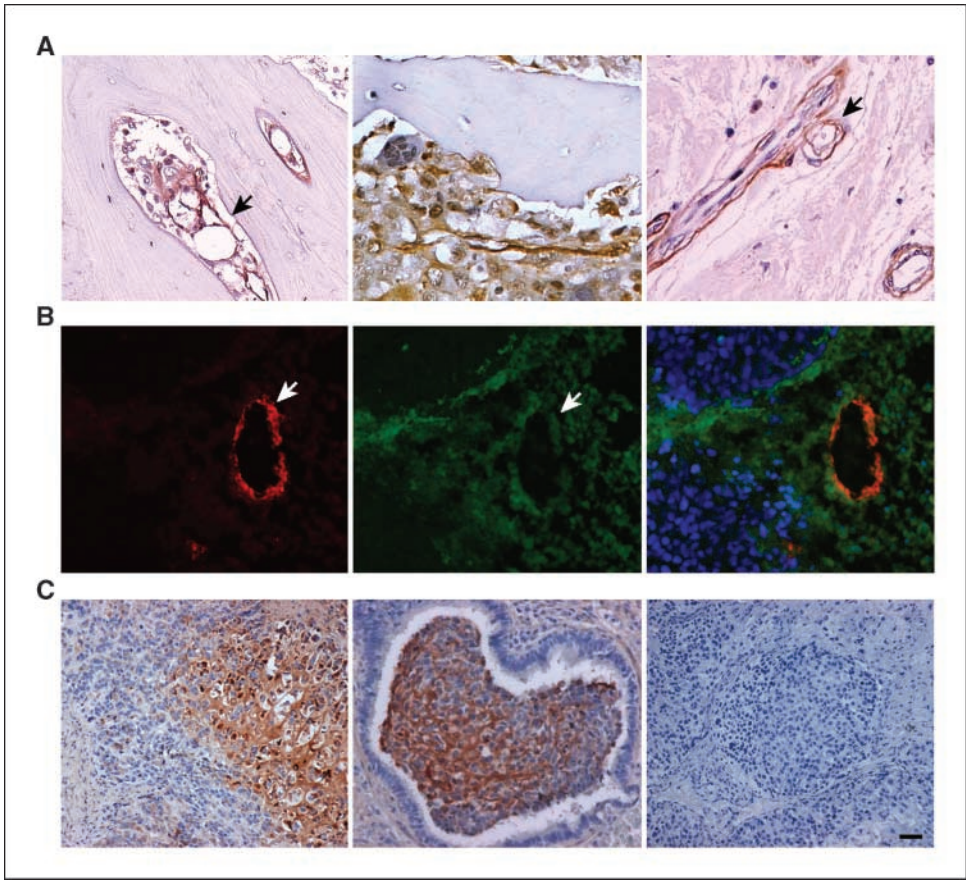

Figure 4. Immunohistochemical staining of IL-11Rα protein in human osteosarcoma biopsy samples and lung metastases. *A,* osteosarcoma cells present in Haversian canals (*left*) and the endothelial lining of small diameter blood vessels (*middle* and *right*) stain positively for IL-11Rα (*arrows*). No staining was observed in the bone. *B,* immunofluorescence detection of IL-11Rα in human osteosarcoma tumor vasculature showed localization of CD31 (*left*; *arrows*), IL-11Rα (*middle*; *arrows*), and colocalization (*right*) in human osteosarcoma. *C,* tumor cells positively express IL-11Rα, whereas the normal lung parenchyma was negative (*left*). Intense staining of osteosarcoma cells was also observed in a bronchiole of the lung (*middle*) with control staining appearing negative (right). *Scale bar,* 80 μm.

independent of the displayed peptide. This selective targeting of the IL-11 mimic phage upon i.v. administration indicates not only that IL-11Rα is accessible to circulating agents but also suggests that therapeutic agents with this ligand-directed system may yield improved targeted agents.

IL-11Rα protein is markedly expressed in primary and metastatic human osteosarcoma. To evaluate whether expression of IL-11Rα in the murine tumor models translates to human osteosarcoma, we first identified a large panel of human tumors in which the samples had <60% necrosis on pathology (n = 30). From this set, we performed immunohistochemical analysis of IL-11Rα expression and scored the staining intensity and distribution (Supplementary Fig. S1; Fig. 4*A*). Moderate-to-high intensity staining of the tumor cells was noted in all primary osteosarcoma samples, with an average score of 2.49 and was tightly distributed with an average score of 2.37 (Supplementary Fig. S1; Fig. 4*A*). Endothelial expression of IL-11Rα within the tumors was seen in >50% of tumor blood vessels and again showed moderate to high intensity staining (average, 2.53; Supplementary Fig. S1; Fig. 4*B*). To confirm endothelial cell localization, we costained IL-11Rα with the endothelial cell marker CD31 (Fig. 4*B*). Of note, only the small caliber blood vessels within the tumor positively expressed the receptor, whereas large tumor blood vessels did not express IL-11Rα at detectable levels; the reason for this observation remains unclear.

We next set out to evaluate whether IL-11Rα expression was maintained in lung metastatic tumors (n = 19). All pulmonary metastases were positive for IL-11Rα, revealing a high intensity of staining with an average of 3.0 and a moderate distribution of 2.84 (Supplementary Fig. S1; Fig. 4*C*). The control normal lung parenchyma was negative for IL-11Rα protein expression. Taken together, therapeutic targeting of IL-11Rα could potentially act as an antitumor, antiangiogenesis, and antimetastatic agent for the management of human osteosarcoma.

In summary, treatment options and survival outcomes of patients with osteosarcoma has all but plateaued over the past 20 year. The discovery of functional ligand receptor systems is a critical first step in the development of new targeted agents. Our histologic and functional findings establish that the IL-11/IL-11Rα system acts as a bona fide ligand receptor pair in osteosarcoma. Moreover, the vascular expression, systemic targeting, and human translation further support the candidacy of IL-11/IL-11Rα–based therapies or imaging agents for osteosarcoma patients.

Disclosure of Potential Conflicts of Interest

No potential conflicts of interest were disclosed.

Acknowledgments

Received 12/19/2008; accepted 12/29/2008; published OnlineFirst 02/24/2009.

Grant support: UT MDACC Institutional Research Grant (V. Lewis), the Robert Wood Johnson Foundation (V. Lewis), the NIH (R. Pasqualini and W. Arap), the DOD (R. Pasqualini and W. Arap), the Gillson-Longenbaugh Foundation (R. Pasqualini and W. Arap), and the Marcus Foundation (R. Pasqualini and W. Arap). We also thank James A. Ragan and family for support of the article.

The costs of publication of this article were defrayed in part by the payment of page charges. This article must therefore be hereby marked *advertisement* in accordance with 18 U.S.C. Section 1734 solely to indicate this fact.

We thank Drs. Marina Cardó-Vila, Su-Feng Ja, and Amado Zurita for technical support, Drs. Michael O'Reilly, Raphael Pollock, and Eugenia Kleinerman for helpful discussions, and Drs. E. Helene Sage and Richard L. Sidman for critical reading of the manuscript.

References

1. Jemal A, Siegel R, Ward E, et al. Cancer statistics, 2006. CA Cancer J Clin 2006;56:106–30.
2. Benjamin R, Chawla S, Murray J, et al. Preoperative chemotherapy for osteosarcoma: a treatment approach facilitating limb salvage with major prognostic indications. In: Jones S, Salmon S, editors. Adjuvant therapy of cancer IV. Philadelphia: Grune and Strattonl 1984. p. 601–10.
3. Hudson M, Jaffe MR, Jaffe N, et al. Pediatric osteosarcoma: therapeutic strategies, results, and prognostic factors derived from a 10-year experience. J Clin Oncol 1990;8:1988–97.
4. McGary EC, Weber K, Mills L, et al. Inhibition of platelet-derived growth factor-mediated proliferation of osteosarcoma cells by the novel tyrosine kinase inhibitor STI571. Clin Cancer Res 2002;8:3584–91.
5. Raile K, Hoflich A, Kessler U, et al. Human osteosarcoma (U-2 OS) cells express both insulin-like growth factor-I (IGF-I) receptors and insulin-like growth factor-II/mannose-6-phosphate (IGF-II/M6P) receptors and synthesize IGF-II: autocrine growth stimulation by IGF-II via the IGF-I receptor. J Cell Physiol 1994;159:531–41.
6. Mansky PJ, Liewehr DJ, Steinberg SM, et al. Treatment of metastatic osteosarcoma with the somatostatin analog OncoLar: significant reduction of insulin-like growth factor-I serum levels. J Pediatr Hematol Oncol 2002;24:440–6.
7. Anderson PM, Wiseman GA, Dispenzieri A, et al. High-dose samarium-153 ethylene diamine tetramethylene phophonate: low toxicity of skeletal irradiation in patients with osteosarcoma and bone metastases. J Clin Oncol 2002;20:189–96.
8. Heiner JP, Miraldi F, Kallick S, et al. Localization of GD2-specific monoclonal antibody 3F8 in human osteosarcoma. Cancer Res 1987;47:5377–81.
9. Modak S, Kramer K, Gultekin SH, Guo HF, Cheung NK. Monoclonal antibody 8H9 targets a novel cell surface antigen expressed by a wide spectrum of human solid tumors. Cancer Res 2001;61:4048–54.
10. Aird WC. Phenotypic heterogeneity of the endothelium: I. structure, function, and mechanisms. Circ Res 2007;100:158–73.
11. Aird WC. Phenotypic heterogeneity of the endothelium: II. Representative vascular beds. Circ Res 2007;100:174–90.
12. Ozawa MG, Zurita AJ, Dias-Neto E, et al. Beyond receptor expression levels: the relevance of target accessibility in ligand-directed pharmacodelivery systems. Trends Cardiovasc Med 2008;18:126–32.
13. Arap W, Kolonin MG, Trepel M, et al. Steps toward mapping the human vasculature by phage display. Nat Med 2002;8:121–7.
14. Pentz RD, Flamm AL, Pasqualini R, Logothetis CJ, Arap W. Revisiting ethical guidelines for research with terminal wean and brain-dead participants. Hastings Cent Rep 2003;33:20–6.
15. Pentz RD, Cohen CB, Wicclair M, et al. Ethics guidelines for research with the recently dead. Nat Med 2005;11:1145–9.
16. Cardó-Vila M, Zurita AJ, Giordano RJ, et al. A ligand peptide motif selected from a cancer patient is a receptor-interacting site within human interleukin-11. PLoS ONE 2008;3:e3452.
17. Zurita AJ, Troncoso P, Cardó-Vila M, et al. Combinatorial screenings in patients: the interleukin-11 receptor α as a candidate target in the progression of human prostate cancer. Cancer Res 2004;64:435–9.
18. Kang Y, Siegel PM, Shu W, et al. A multigenic program mediating breast cancer metastasis to bone. Cancer Cell 2003;3:537–49.
19. Berlin O, Samid D, Donthineni-Rao R, Akeson W, Amiel D, Woods VL, Jr. Development of a novel spontaneous metastasis model of human osteosarcoma transplanted orthotopically into bone of athymic mice. Cancer Res 1993;53:4890–5.
20. Hanavadi S, Martin TA, Watkins G, Mansel RE, Jiang WG. Expression of interleukin 11 and its receptor and their prognostic value in human breast cancer. Ann Surg Oncol 2006;13:802–8.
21. Mohamedali KA, Kedar D, Sweeney P, et al. The vascular-targeting fusion toxin VEGF121/rGel inhibits the growth of orthotopic human bladder carcinoma tumors. Neoplasia 2008;7:912–20.
22. Arap W, Pasqualini R, Ruoslahti E. Cancer treatment by targeted drug delivery to tumor vasculature in a mouse model. Science 1998;279:377–80.
23. Kolonin MG, Saha PK, Chan L, Pasqualini R, Arap W. Reversal of obesity by targeted ablation of adipose tissue. Nat Med 2004;10:625–32.
24. Arap MA, Lahdenranta J, Mintz PJ, et al. Cell surface expression of the stress response chaperone GRP78 enables tumor targeting by circulating ligands. Cancer Cell 2004;6:275–84.
25. Luu HH, Kang Q, Park JK, et al. An orthotopic model of human osteosarcoma growth and spontaneous pulmonary metastasis. Clin Exp Metastasis 2005;22:319–29.
26. Rajotte D, Arap W, Hagedorn E, Koivunen E, Pasqualini R, Ruoslahti E. Molecular heterogeneity of the vascular endothelium revealed by *in vivo* phage display. J Clin Invest 1998;102:430–7.
27. Pasqualini R, Koivunen E, Ruoslahti E. Alpha v integrins as receptors for tumor targeting by circulating ligands. Nat Biotechnol 1997;15:542–6.